



HAL
open science

The measurement of water transport in porous materials using impedance spectroscopy

R J Ball, G C Allen

► **To cite this version:**

R J Ball, G C Allen. The measurement of water transport in porous materials using impedance spectroscopy. *Journal of Physics D: Applied Physics*, 2010, 43 (10), pp.105503. 10.1088/0022-3727/43/10/105503 . hal-00569551

HAL Id: hal-00569551

<https://hal.science/hal-00569551>

Submitted on 25 Feb 2011

HAL is a multi-disciplinary open access archive for the deposit and dissemination of scientific research documents, whether they are published or not. The documents may come from teaching and research institutions in France or abroad, or from public or private research centers.

L'archive ouverte pluridisciplinaire **HAL**, est destinée au dépôt et à la diffusion de documents scientifiques de niveau recherche, publiés ou non, émanant des établissements d'enseignement et de recherche français ou étrangers, des laboratoires publics ou privés.

The measurement of water transport in porous materials using impedance spectroscopy

R J Ball and G C Allen

Interface Analysis Centre, University of Bristol, Oldbury House, 121 St Michael's, Hill, Bristol, BS2 8BS

Short title: Measurement of water transport in porous materials using impedance spectroscopy

Classification numbers:

Abstract

This paper describes the application of electrical measurements to monitor the extraction (movement of water from the mortar) of water from calcium lime, natural hydraulic lime and Portland cement mortars placed on an adsorbent brick substrate. Impedance measurements were used to identify the changes in bulk resistance of the mortar. A model has been developed combining sharp front theory and Boltzmann's distribution law of statistical thermodynamics to identify the point at which no further absorption of water in to the brick occurs. A linear relationship was found between the exponential of bulk resistance and square root of time during dewatering. A change in gradient was attributed to the end of dewatering.

Key words: mortar, dewatering, impedance spectroscopy

1. Introduction

In their pioneering publication Hall and Hoff (2002) observed that "If there is a science of building the interplay of water and materials must be one of its themes". The water level in a normal stone wall is determined by the rate of absorption and evaporation which in turn depends on the porosity of the stone. Thus the movement of water through

building materials, especially brick structures, may be a limiting factor not only in their durability but also in process of their construction. Climatic changes in the environment will lead to buildings experiencing periods of wetting and drying where the measurement and calculation of the transport of vapour and liquid water is essential for the understanding of their deterioration and restoration.

This paper describes the application of electrical measurements to monitor the dewatering and drying of the mortar materials calcium lime, natural hydraulic lime (NHL) (Allen *et al* 2003) and Portland cement (Bye 1983) mortars used in the bonding of absorbent brick substrates. Previously impedance spectroscopy has been applied to cement mortars to study rapid hydration reactions (McCarter *et al* 2000) but lime mortars stiffen in an entirely different way where the main reaction involves the absorption of CO₂ following hydration (Van Balen 2005). For this reason dewatering becomes especially important. Carbonation is encouraged in moist rather than saturated materials and is governed by the relative humidity (El-Turki *et al* 2007, El-Turki *et al* 2009)

In this study a model has been developed combining sharp front theory (Collier *et al* 2007) and Boltzmann's distribution law of statistical thermodynamics to estimate the rate of dewatering from the recorded changes in bulk resistance. In the experiments a mortar of suitable thickness was chosen to allow the rate of desorption to be carefully studied in detail. This allowed the initial rapid dewatering stage and the subsequent slower rate of diffusion to be assessed when the remaining concentration of water had fallen to a level determined by the capillary action of the substrate.

2. Experimental Method

2.1 Sample preparation

Single rather than hybrid mortars were manufactured from a pure calcium lime (CL90), natural hydraulic lime (NHL3.5) and Portland cement individually. These materials were supplied by Hanson Cement Ltd, Clitheroe, Lancashire, UK. The oxide composition, determined by X-ray fluorescence spectroscopy (XRF), of the calcium lime (CL90) and Portland Cement was reported by A El-Turki *et al* (2009) and that of

the NHL3.5 by Ball and Allen (2009). The bulk densities of the CL90, NHL3.5 and OPC binders used were 650.6, 666.3 and 1119.3 kgm⁻³ respectively. The manufacturers recommended volume ratio for binder to aggregate of 0.5 and water to binder of 0.78 was used in all cases. A quarried Croxden sand composed of mainly silicon with traces of aluminium, potassium, titanium, iron and calcium of bulk density 1475.5 kgm⁻³ was used as aggregate. Its particle size distribution and energy dispersive X-ray analysis was reported by Ball and Allen (2009). The dry constituents of each mortar type were intimately mixed before the water was added, prior to further mixing. Due to the small quantities of mortar required for each experiment all mixing was done by hand for 5 minutes following the addition of water. After mixing the mortar was immediately applied to the brick and the experiment initiated within 1 minute.

2.2 Substrate sorptivity

Mortars were set upon square section brick prisms of width 25 mm and length 80 mm, sufficient to fully dewater the depth of mortar applied. Prisms were cut from golden purple bricks supplied by Istock Brick Ltd, Roughdales Factory. The sorptivity of each prism was determined using the method described by Hall *et al* (1986). Prior to measurement prisms were oven dried at 105 °C for at least 12 hours. The weight of each piece of brick was measured, to an accuracy of 0.1 g, at time intervals of 1, 2, 4, 9, 16 and 25 minutes when the bottom face was in contact with a shallow layer of water. Brick pieces were dried again in the oven under the same conditions before the mortar was applied. The volume of water absorbed by the brick at each of the time intervals was calculated from the density of water, 1000 kgm⁻³, and the weight change. Water volume was then plotted against the square root of time and a linear trend line fitted using a least squares algorithm. By dividing the gradient of the line by the cross sectional area of the prism a value of the brick desorptivity, R, was calculated.

2.3 Impedance Spectroscopy

The application of impedance spectroscopy to cementitious systems is well documented (Christensen *et al* 1994). The impedance response of the wet mix was monitored using a Solartron 1260 impedance analyser over the frequency range from 10 MHz - 100 Hz. Each sweep between these frequencies contained 5 steps per decade and were carried

out at a potential of 100 mV. 200 sweeps each lasting 70 seconds were repeated continuously over a time period of 225 minutes. The test cell shown in figure 1 (a) was constructed using two rectangular stainless steel electrodes 25 mm by 30 mm spaced 25 mm apart. These were positioned in a square section tube of the same dimensions as the brick prism to allow unidirectional flow of liquid between the wet mix and substrate. The electrodes were positioned 15 mm above the brick surface.

3. Theory

The dewatering of mortar in contact with an absorbent substrate can be analysed using the sharp front model developed by Hall and Hoff (2002). This model describes the relationship between the sorptivity, S , of the substrate, the desorptivity, R , of the slurry and the transfer sorptivity, A , between the slurry and the substrate. The withdrawal of water from a wet mix by an initially dry substrate occurs by capillary forces. The slurry can be divided into a ‘filter cake’ and ‘wet mix’ as shown in figure 1 (b). As dewatering progresses the thickness of filter cake increases until no wet mix remains or the brick substrate becomes completely saturated. The application of Darcy’s law to the filter cake yields equation 1.

$$\frac{di}{dt} = -K_c \frac{\Psi_i}{L_c} = -K_c \frac{\alpha \Psi_i}{\beta i} \quad 1$$

Where i (m) is the cumulative volume of water desorbed per unit area of wet mix, t (s) is time, K_c (ms^{-1}) is the permeability of the cake, Ψ_i (MPa) is the capillary potential, L_c (m) is the depth of the cake, and, α and β , are terms relating to the volume fraction of water. i can be defined by equation 2 in terms of the cumulative volume of water adsorbed, V_{H_2O} (m^3) and the area of the wet mix in contact with the substrate, A_{sub} (m^2).

$$i = \frac{V_{H_2O}}{A_{sub}} \quad 2$$

Integration of equation 1 gives equation 3.

$$i = \left(\frac{2K_c |\Psi_t| \alpha}{\beta} \right)^{\frac{1}{2}} t^{\frac{1}{2}} = R_{wm} t^{\frac{1}{2}} \quad 3$$

Alternatively if the area of the brick substrate, A_{sub} , is represented by a capillary of radius, r , the flow of water can be described using the Washburn equation, equation 4 (Washburn 1921).

$$v = \frac{dh}{dt} = \frac{r\gamma \cos \theta}{4\eta h} - \frac{r^2 \rho g}{8\eta} \quad 4$$

Where h is the depth of water adsorbed into the brick, $\gamma \cos \theta$ is the surface tension and η is viscosity. Integration of this equation ignoring the gravity term yields equation 5.

$$h^2 = \frac{\gamma r \cos \theta}{2\eta} t \quad 5$$

Recognising that the term, i , used in sharp front theory (equation 2) is comparable with h , rearranging this equation gives a $t^{\frac{1}{2}}$ relationship similar to that of equation 3, as shown in equation 6. However in this case the flow is described by the properties of the brick substrate and not the wet mix.

$$h = \left(\frac{\gamma r \cos \theta}{4\eta} \right)^{\frac{1}{2}} t^{\frac{1}{2}} \quad 6$$

If the initial volumetric water content of the mix at $t = 0$ is w_0 then the water content at time t , w , is given by equation 7.

$$w = w_0 - iA_{sub} \quad 7$$

The mortar can be described as a system where solid particles of binder or aggregate are suspended in a liquid. The potential energy of ions dissolved in the liquid can be related

to the number of ions by applying Boltzmann's distribution law of statistical thermodynamics, equation 8 (Besanson 1974).

$$\frac{N_i}{N_j} = \exp\left[-\frac{(E_i - E_j)}{kT}\right] \quad 8$$

Where N_i and N_j are the numbers of constituent ions in states i and j and E_i and E_j are the respective potential energies, k is the universal constant equal to $1.38041 \times 10^{-23} \text{ JK}^{-1}$; and T is temperature, K .

When a solid with a charged surface is in contact with a liquid, containing ions, a double layer is formed. This comprises a tightly bound layer of fairly immobile ions adjacent to the solid and an oppositely charged ionic atmosphere (Dukhin and Dejaguin 1974). If stage i corresponds to ions within the double layer and stage j to those in the bulk water, then the difference in energy between the two states can be expressed in terms of the electrical Maxwell forces defined by equation 9.

$$E_i - E_j = ze(\varphi_i - \varphi_j) \quad 9$$

where φ is the electrical potential; e is the electronic charge; z is the summary valence of the mobile ions in the solution (Neilsen *et al* 1972). By combining equations 8 and 9 the fraction N_i/N_j representing the relative number of mobile electrical charges in the bulk water and double layer is obtained, equation 10:

$$\frac{N_i}{N_j} = \exp\left[-\frac{ze(\varphi_i - \varphi_j)}{kT}\right] \quad 10$$

If the number of ions in the double layer, N_i , is assumed to be constant and those in the bulk water, N_j , is proportional to the water content the ratio, N_i/N_j , is proportional to water content. The electrical potential difference $\varphi_i - \varphi_j$ is proportional to the mortar bulk resistance according to Ohm's law. Thus, from equation 7 a relationship between mortar pore water content, w , and electrical resistance can be obtained, equation 11, where a

and b are empirical parameters and R_b is the resistivity. It should be noted that parameter b is temperature dependent.

$$w = a \exp(-bR_b) \quad 11$$

Substitution of equations 3 and 11 into equation 7 gives equation 12.

$$a \exp(-bR_b) = w_0 - A_{sub} R_{wm} t^{\frac{1}{2}} \quad 12$$

Equation 12 can be re-arranged into the form, equation 13.

$$\exp(-bR_b) = -\frac{A_{sub} R_{wm}}{a} t^{\frac{1}{2}} + \frac{w_0}{a} \quad 13$$

This equation predicts that if b , A_{sub} , R_{wm} , a and w_0 are constants a plot of exponential of $(-b R_b)$ versus square root of time will be linear.

4. Results

Values of brick sorptivity for each of the prisms used are shown in table 1, ranging between 2.2 and 2.6 mm min^{0.5}. Such variations are typical for the type of brick used and close enough to allow meaningful comparison between the mortars tested.

A typical complex plane plot for the CL90 mortar after a period of 30 minutes is shown in figure 2 (a). The plot comprises two arcs which correspond to the mortar (left arc) and electrodes (right arc). The intersection of the arcs with the x-axis (real impedance) occurred at a frequency of 63 kHz and corresponds to the bulk resistance, R_b . The intersection also occurred at this frequency for the natural hydraulic and cement mortars. An idealised plot and equivalent circuit diagram is shown in figure 2 (b).

Figure 3 shows plots of exponential of $(-bR_b)$ versus square root of time for the calcium lime, natural hydraulic lime and Portland cement mortars respectively. A value of $-0.001 \text{ J}^{-1} \text{ A}^2 \text{ s}$ was used for b . A linear trend line was fitted to the beginning and end

sections of data from each specimen. In each case a correlation coefficient of 0.99 was obtained.

The gradient of the initial section of the curve corresponding to dewatering is given in table 1. An increase in gradient was observed with mortar type from calcium lime, natural hydraulic lime and Portland cement mortars respectively.

5. Discussion

The mechanisms by which water is retained in mortars, plasters and renders in the wet mix will depend on their water content. This may take the form of free flowing water at complete saturation and physically bound water when surface tension effects become dominant. This approach has been reported previously by Zacharopoulou (2006) for lime putties.

The results presented here are those for mortars containing calcium lime, natural hydraulic lime and Portland cement binders. Figure 3 illustrates plots of the exponential of the recorded resistivity versus the square root of time. These may be analysed in terms of two regions relating to the mode of extraction of unbound or free flowing water. The initial slope describes the absorption of liquid from the wet mortar mixture into the brick by capillary forces and is governed by the chemical changes taking place. This may be expressed by sharp front theory to derive an equation for the time taken to dewater a wet mortar by an absorbent substrate. (C Ince *et al* 2009). As with Ficks law the rate at which the mix loses water depends on its thickness and assumes no restriction between the media involved in the transfer process giving a clear delineation at its endpoint.

Unfortunately though the inhomogeneous nature of the mortar brought about by the imperfect distribution of water, aggregate and binder and the variable composition of the adsorbate brick greatly complicates the dewatering process producing a less well defined endpoint. In the present study it is assumed that the change in gradient of the resistivity – time curve, shown in Figure 4, signifies a change in the dewatering process. The extent of this inhomogeneity is reflected by the time over which the change in gradient (transition) occurs.

When the slopes of the lines and the time at which the change in slope occurs are compared it is apparent that the type of binder used in the mortar has an important influence on behaviour. It is noteworthy that the steepest gradient was observed for the Portland cement mortar which contained the highest proportion of reactive hydraulic phases and where the chemical activity was greatest. Especially noteworthy was that in this measurement there was an indistinct change in gradient and hence little evidence of a two stage process. Moreover the conductance measurements reported by McCarter and Garvin (1989) also showed little change in gradient with changing water content in cement phases. Here dewatering appeared to be essentially continuous but the period of this process was longer than that for the natural hydraulic and calcium lime. This observation may be due to the fact that with Portland cement the rapid hydraulic reaction forms a silicate network through which the remaining free water must be progressively extracted with increased tortuosity.

In the case of CL90 the main setting reaction, carbonation, does not occur to any significant extent within the duration of the experiment. The absence of a structural network does not provide an increasingly restricted path thereby allowing a more rapid extraction of water. By contrast, for the natural hydraulic lime a very significant change in gradient was observed giving a very clear indication of the processes involved. Initially the hydraulic reaction from the incorporated dicalcium silicate phase produced a loose network of a gelatinous hydrated silicate limiting the process of free water extraction. At the intercept the remaining incorporated water is more tightly bound and the rate of the dewatering process is dramatically altered. It is possible that the loosely bound silicate gelatinous network may be drawn towards the mortar brick interface. Experiments with NHL3.5 mortars dewatered on a brick substrate have identified a crystalline silicate layer at the surface of the substrate.

Clearly impedance measurements may give an indication of the time required to dewater the sample. Previous research (El-Turki *et al* 2009) has highlighted the importance of dewatering on the subsequent mechanical properties of a mortar. Knowledge of the dewatering time is of importance to the construction industry. This study provides an important method of measuring dewatering and subsequent water loss of a wet mix. Its application to mortars in-service would allow their subsequent

mechanical properties, following stiffening, to be assessed. The bulk resistance of the mortar during and after dewatering will be influenced by factors such as the type and concentration of ions within the mix water. This is a function of the type of binder where cementitious binders, such as Portland cement, will contain a higher proportion of ions such as Cl^- compared to calcium lime. The surface energy of the solid phases is also expected to influence the electrical characteristics of a mix. Consideration of these effects will become more significant particularly as more exotic additives derived from low embodied energy materials and industrial wastes become increasingly prevalent.

6. Conclusions

The results show a decrease in the exponential of $(-bR_b)$ with square root of time for the mortars examined. This is consistent with a decrease in conductivity with loss of water and confirms that conduction is through the liquid as opposed to solid phase.

The time at which the change in slope occurs suggests the flow of water into the brick is controlled by the type of binder used to make the mortar.

The results demonstrate the ability of impedance spectroscopy to determine mortar bulk resistance and relate this to water flow into a brick.

7. Acknowledgements

The authors would like to thank the EPSRC for funding this work and Castle Cement and Ibstock Brick for supply of materials. Thanks are also due to Margaret Carter and Moria Wilson for helpful discussions.

8. References

Allen G C, Allen J, Elton N, Farey M, Holmes S, Livesey P and Radonjic M, 2003
Hydraulic Lime Mortar for Stone, Brick and Block Masonry, Donhead Publishing Ltd, Shaftesbury, Dorset, ISBN: 1873394640

- Ball R J and Allen G C 2009 *Int. J. Sustain. Develop.* iFirst article, 1-7
- Besanson R.M (ed. 1) 1974. *The Encyclopedia of Physics* (Van Nostrand Reinhold Comp. NY), ISBN 0442005229, 80-81
- Bye G C 1983 *Portland Cement* (Pergamon Press, Oxford), ISBN 0080299644
- Christensen B J, Coverdale R T, Olson R A, Ford S.J, Garboczi E J, Jennings H M and Mason T 1994 *J. Am. Ceram. Soc.* **77** 2789-804
- Collier N C, Wilson M A, Carter M A, Hoff W D, Hall C, Ball R J, El-Turki A and Allen G C 2007 *J. Phys. D.* **40** 13 4049-4054
- Dukhin S S and Derjaguin B V 1974 *Electrokinetic Phenomena* (J.Wiley and Sons)
- El-Turki A, Ball R J and Allen G C 2009 *J. Am. Ceram. Soc.* Submitted for publication
- El-Turki A, Ball R J, Holmes S and Allen G C 2009 *Const. and Build. Mat.* Submitted for publication
- El-Turki A, Carter M A, Wilson M A, Ball R J and Allen G C 2009 *Const. and Build. Mat.* **23** 1423-1428
- El-Turki A, Ball R J and Allen G C 2007 *Cem. Con. Res.* **37** 1233 - 1240
- Nielsen D R, Jackson R D, Cary J W and Evans D D 1972 *Soil Water. ASA (American Society of Agronomy), SSSA (Soil Science Society of America)* (677 South Segoe Road, Madison, Wisconsin, 53711).
- Hall C and Hoff W D 2002 *Water Transport in Brick, Stone and Concrete* (London: Taylor and Francis), ISBN 0-419-22890-X
- Hall C and Tse T K M 1986 *Bldg. Env.* **21** 113-118
- Ince C, Carter M A, Wilson M A, El-Turki A, Ball R J, Allen G C and Collier 2009 N C, *Mat. Struct.* DOI 10.1617/s11527-009-9560-5
- McCarter W J, Starrs G and Chrisp T M 2000 *Cem. Con. Res.* **30** 1395 – 1400
- McCarter W J and Garvin S 1989 *J. Phys. D.* 1773-1776
- Van Balen K 2005 *Cem. Conc. Res.* **35** 647
- Washburn E W 1921 *Phys. Rev.* **17** 273 – 283
- Zacharopoulou G 2006 *J. Build. Lime. Forum* **13** 88

Tables

Table 1. Values calculated from the experimental data relating to calcium lime, natural hydraulic lime (NHL) 3.5 lime and Portland cement mortars dewatered on Ibstock golden purple brick prisms.

	CL90	NHL3.5	PC
Brick sorptivity, S , $\text{mm s}^{0.5}$	2.4	2.2	2.6
Gradient of dewatering line [$\times 10^{-2}$]	3.5	4.4	4.8
Square root of dewatering time, $t^{0.5}$, $\text{min}^{0.5}$	5.7	6.4	7.7
Dewatering time (intercept of lines), min	32	42	60

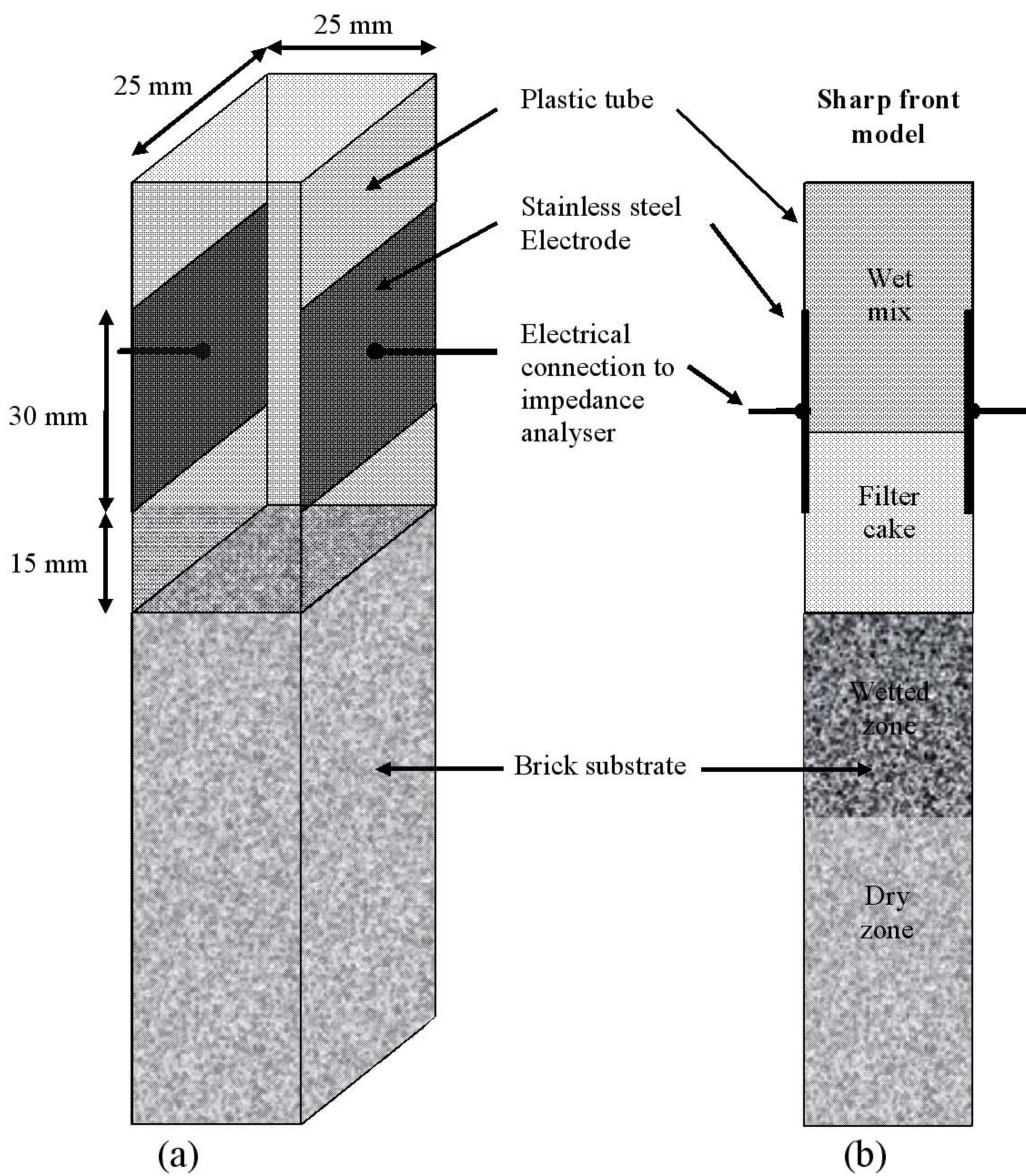
List of Figure captions

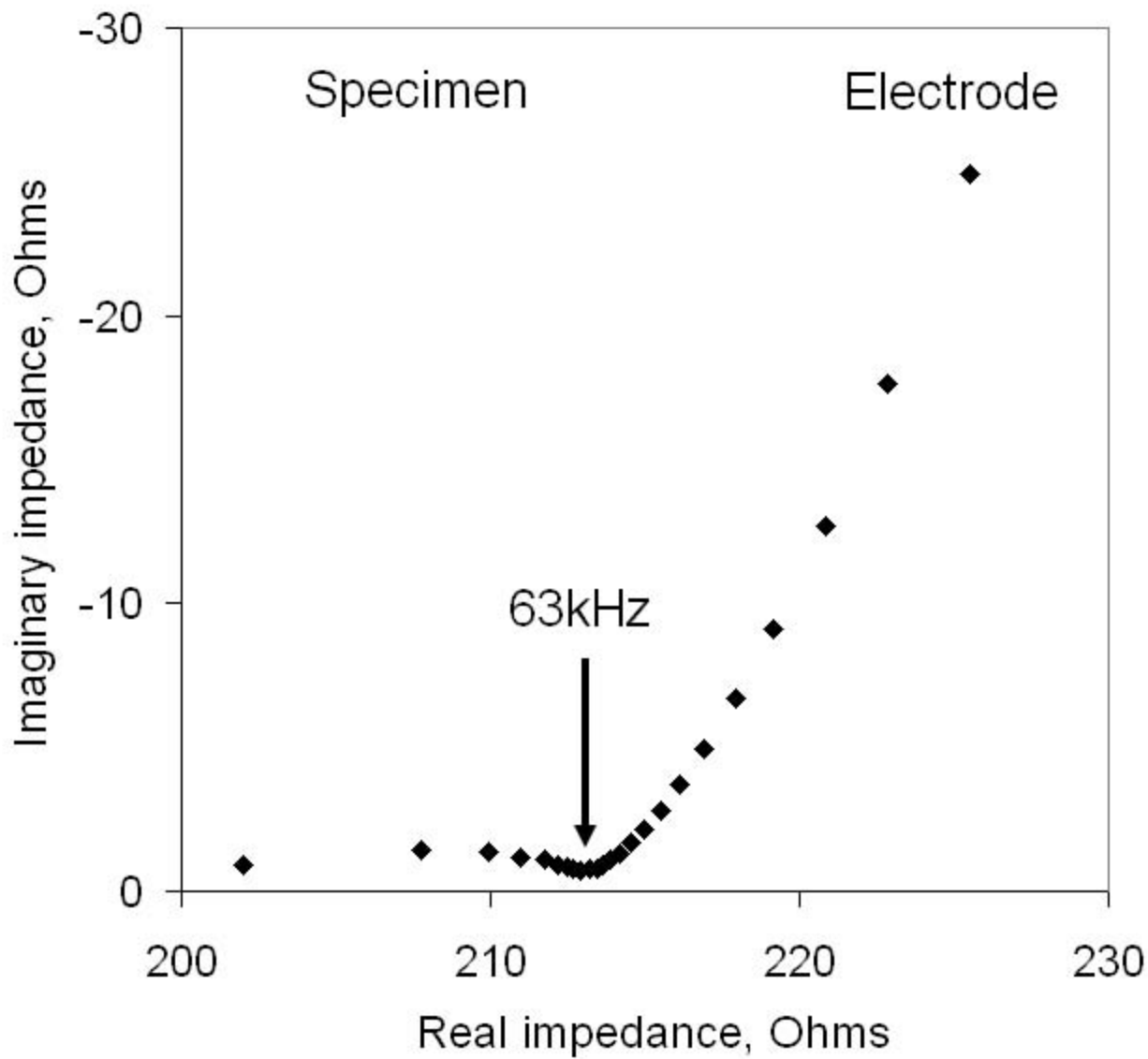
Figure 1. Experimental setup (a) Schematic diagram showing test cell, electrodes and brick prism. (b) Sharp front model of dewatering mortar.

Figure 2. (a) Complex plane plot obtained after 30 minutes of dewatering for a calcium lime mortar showing the bulk resistance corresponds to a frequency of 63 kHz. (b) idealised complex plane plot and equivalent circuit model.

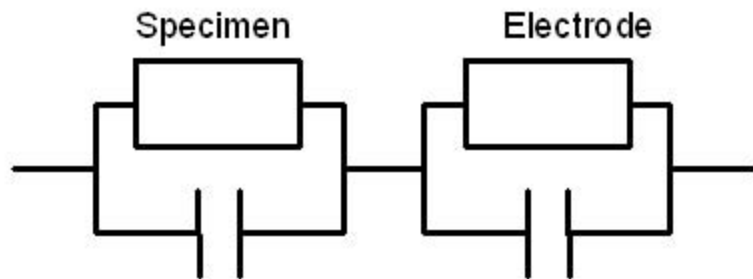
Figure 3. Plots of exponential of $(-b R_b)$ versus square root of time for Portland cement, natural hydraulic lime and calcium lime mortars showing two distinct linear regions.

Figure 4. Typical exponential of $(-b R_b)$ versus square root of time plot showing idealised structures for free and physically bound water.





Equivalent circuit



Imaginary impedance, Ohms

